

Electronic structure of T_5T_9 metallic glasses ($T_5 = \text{Nb, Ta}$; $T_9 = \text{Rh, Ir}$) studied by photoelectron spectroscopy

A. DasGupta,* P. Oelhafen,[†] U. Gubler, R. Lapka, and H.-J. Güntherodt
Institut für Physik, Universität Basel, CH-4056 Basel, Switzerland

V. L. Moruzzi and A. R. Williams
IBM Thomas J. Watson Research Center, Yorktown Heights, New York 10598
(Received 21 September 1981)

Photoelectron spectroscopy of glassy $\text{Nb}_{55}\text{Rh}_{45}$, $\text{Nb}_{55}\text{Ir}_{45}$, $\text{Ta}_{55}\text{Rh}_{45}$, and $\text{Ta}_{55}\text{Ir}_{45}$ alloys reveal a common d band of the two alloy constituents with a large shift of the T_9 metal d states to higher, and a shift of the T_5 metal d states to lower binding energies relative to the corresponding pure metal. The charge transferred from the T_5 to T_9 metal on alloying is quite small and results in a small (positive and negative) binding-energy shift of the core electrons of the T_9 metal.

INTRODUCTION

The metallic glasses in the T_5T_9 transition-metal alloy system ($T_5 = \text{Nb, Ta}$; $T_9 = \text{Rh, Ir}$) are characterized by very high glass-to-crystalline transition temperatures, T_x , with some as high as 1065 °C.^{1,2} One of the first known members of this binary-alloy series was a Nb-Rh alloy, which exhibited superconducting properties.³ More recently, the eutectic temperature, elastic modulus, microhardness, H_V , and superconducting properties of the series have been studied and correlated with T_x .¹ The aim of this present work is to understand the electronic contributions to the thermal stability and formation of these alloys and to understand the characteristics of the electronic structure responsible for their superconducting properties.

This paper is organized in two sections. First, we present our experimental results which include the first x-ray photoelectron spectroscopy (XPS) and ultraviolet photoelectron spectroscopy (UPS) studies of the binary alloys $(T_5)_{55}(T_9)_{45}$. This composition corresponds approximately to the eutectic composition. In the second section, we utilize partial- and total-state densities computed self-consistently for related ordered compounds to understand the electronic structure of these metallic glasses.

EXPERIMENTAL RESULTS

The T_5T_9 metallic glasses reported in this study were prepared in a manner described elsewhere.² Alloy buttons of approximately 3 g in weight were

prepared by arc-melting weighed amounts of the pure constituent elements in a copper hearth under an argon atmosphere. Small portions of these buttons, approximately 30 mg in weight, were quenched from the liquid state using an arc-hammer furnace. The resultant samples, about 1 cm in diameter and 20–30 μm in thickness, were used in the investigations after cropping off edge sections which were often found to be crystalline. X-ray diffraction was used to ensure the amorphous nature of the samples.

The photoelectron spectra were measured with a Leybold-Heraeus electron spectrometer EA 10/100. The UPS data were obtained by operating the energy analyzer in the constant sensitivity mode with a retardation factor of 3 and the XPS measurements were performed in the constant-resolution mode with a pass energy of 50 eV. The resulting energy resolutions for the different excitation energies were 0.1 eV (for $h\nu = 16.8$ eV, 21.2 eV), 0.17 eV (for $h\nu = 40.8$ eV), and 0.9 eV (for $h\nu = 1253.6$ eV). No satellite or background subtraction has been applied to the spectra presented in this study. The measurements were performed at a residual gas pressure in the 10^{-11} -torr range. During the UPS measurements the gas pressure was in the lower 10^{-9} torr for Ne I, He I radiation and in the upper 10^{-10} -torr range for He II radiation.

The samples were cleaned by Ar-ion bombardment in two steps: by sputtering with a penning ion gun (IQP10/63 Leybold-Heraeus) in a sample preparation chamber, typically for 20 min with a primary energy of 3.5 keV and with a scanning ion gun (IQE12/63, Leybold-Heraeus) in the measuring

chamber for about 10 min at 5 keV.

Although it turned out to be important to check possible preferential sputtering effects and changes in the surface composition by an alternative cleaning procedure,⁴ the dimensions and the thickness of the samples did not allow mechanical cleaning of the surface. However, the alloy concentrations near the surface deduced from XPS core-level intensities and photoelectron excitation cross sections⁵ were in agreement with the bulk concentration within 10 at. %.

The alloy UPS and XPS measurements were directly compared with the corresponding measurements on the pure constituents by using high-purity polycrystalline foils of Nb, Ta, Rh, and Ir on the same sample holder. This procedure allows us to measure core-level binding-energy shifts with an accuracy better than 0.05 eV.

The valence-band UPS spectra of the four glassy alloys measured with an excitation energy of $h\nu=40.8$ eV are presented in Fig. 1. The main features of the spectra which are dominated by photoelectrons originating from the d bands of the two alloy constituents are the following: (i) The valence-band spectra of the alloys show one distinct peak located about in the center of the valence band. The peak positions for $Nb_{55}Rh_{45}$, $Ta_{55}Rh_{45}$, $Nb_{55}Ir_{45}$, and $Ta_{55}Ir_{45}$ are 2.9, 2.9, 3.3, and 3.5 eV, respectively; the corresponding occupied d -band widths are 5.3, 5.5, 7.3, and 6.8 eV. Note that these alloy spectra are quite different

from those of the pure constituents, which have their d -band maxima near the Fermi level E_F .⁶ (ii) The spectra reveal a weak shoulder near E_F , clearly visible in the $Nb_{55}Rh_{45}$ and $Ta_{55}Ir_{45}$ valence bands. (iii) Other than the main peak and the shoulder near E_F the valence-band spectra consist of smooth curves and do not show any particular structures in contrast to the spectra measured on the crystalline alloy constituents.

Figure 1 shows that the four alloys have similar valence-band properties. We, therefore, would like to discuss one system, namely, the Nb-Rh system, in more detail. Valence-band spectra measured with different excitation energies are shown in Fig. 2 and the corresponding measurements on pure crystalline Rh are presented in Fig. 3. The spectra of $Nb_{55}Rh_{45}$ in Fig. 2 clearly demonstrate the change in the photoelectron excitation cross section for the different d bands when going from the XPS spectrum ($h\nu=1253.6$ eV) to the UPS Ne I spectrum ($h\nu=16.8$ eV). Whereas the XPS and He II spectra are quite similar (note the much lower resolution in the XPS measurements), the lower photon energies emphasize the electron states near E_F . The photoelectron spectra measured with higher photon energies ($h\nu > 40$ eV) are believed to be a better representation of the density of states than those of lower excitation energies because the latter are dominated by strongly energy-dependent matrix elements for optical transition and final states effects.

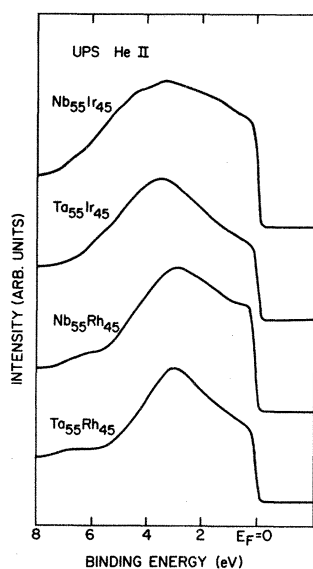


FIG. 1. Valence-band UPS He II ($h\nu=40.8$ eV) spectra of glassy T_5T_9 alloys.

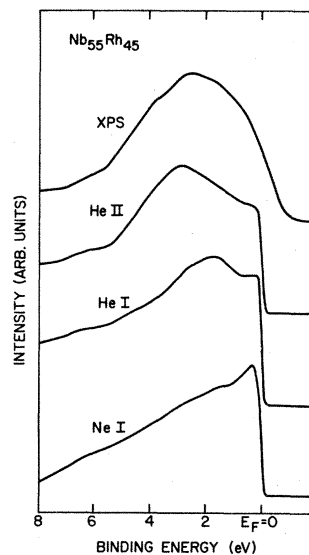


FIG. 2. Valence-band photoelectron spectra of the metallic glass $Nb_{55}Rh_{45}$ measured with different excitation energies: XPS ($h\nu=1253.6$ eV), He II (40.8 eV), He I (21.2 eV), and Ne I (16.8 eV).

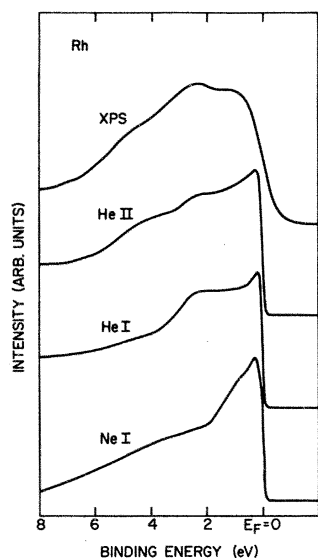


FIG. 3. Valence-band photoelectron spectra of polycrystalline Rh measured with different excitation energies: XPS ($h\nu=1253.6$ eV), He II (40.8 eV), He I (21.2 eV), and Ne I (16.8 eV).

The valence-band spectra of pure polycrystalline Rh in Fig. 3 also demonstrate a strong photon energy dependence. Again, the general trend is a higher sensitivity for electron states near E_F with decreasing photon energy. This means that in measurements with low photon energies the excitation cross section for electrons from the bonding d states in the lower part of the valence band is much smaller than that for the antibonding states near E_F . For higher excitation energies the excitation cross section shows a much weaker binding-energy dependence.

The structures in the XPS, He II, He I spectra at binding energies of 2.4 and 4.6 eV as well as the width of the valence band of about 6 eV is in good agreement with density of states calculations of Moruzzi *et al.*⁷ According to this calculation distinct maxima occur at 2.6 and 4.8 eV and the bottom of the d band is near 6.2 eV.

The core-level binding-energy shifts of the most intense core lines are given in Table I. The Nb $3d_{5/2}$ and Ta $4d_{3/2}$ binding-energy shifts are of the same order of magnitude as those in Nb-Ni and Ta-Ni alloys⁸ and the Rh $3d_{5/2}$ and Ir $4f_{7/2}$ shifts are small. The negative binding-energy shift for the Ir core levels is an exception and has yet to be observed for a group of 17 different transition-metal alloys studied. In addition, all the core-level line shapes show a change towards higher symme-

TABLE I. Core-level binding-energy shifts (in eV) of the most intense lines on alloying. Unless otherwise indicated the given shifts have an accuracy of ± 0.05 eV.

	Nb ₅₅ Rh ₄₅	Ta ₅₅ Rh ₄₅	Nb ₅₅ Ir ₄₅	Ta ₅₅ Ir ₄₅
Nb $3d_{5/2}$	0.77		0.86	
Rh $3d_{5/2}$	0.13	0.27		
Ta $4d_{3/2}$		0.70 ± 0.15		0.85 ± 0.15
Ta $4f_{7/2}$		0.75		0.83
Ir $4f_{7/2}$			-0.27	-0.17

try in alloying. This effect will be discussed in the next section.

DISCUSSION

The density of states of glassy alloys made up of transition-metal constituents are characterized by either common d bands (e.g., Fe-Zr) or split d bands (e.g., Pt-Zr) depending on the difference in the atomic d -level energy or the valence difference of the constituents.^{9,10} In all cases, the d states associated with the late transition-metal constituent (the constituent with the higher d -electron number) dominate the high-binding-energy portion of the common d band. As a consequence, the local d -state density near E_F at the late transition-metal site is strongly reduced and the excitation of electron-hole pairs becomes less probable. This is observed in the form of a decrease of the core-level line asymmetry.¹¹ The effect is clearly visible for the Rh and Ir core lines and less distinct for the Nb and Ta core levels. The decrease of the later core line asymmetries is a consequence of the position of E_F near a maximum in the density of states for pure Nb and Ta.¹²

In contrast, the d states of the early transition-metal constituent dominate the upper portion of the common d -band energies. The electronic structure near E_F is therefore mainly determined by electronic states of the early transition metal. The shoulders near E_F in the UPS spectra of Fig. 1 are attributed mainly to Nb and Ta (early transition-metal constituents).

It has been shown that the valence difference Δn is an important parameter in determining the degree of d -band splitting.^{9,10} The T_5T_9 alloys studied here with a valence difference $\Delta n=4$ compare favorably with previously studied Fe-Zr alloys⁹ which are also essentially common d -band alloys.

Although the general shapes of the bands are similar, the band widths, which correlate with the band widths of the pure late transition-metal constituents are seen to increase in going from Ni to Rh and Ir alloys.

As we have discussed in previous publications,¹¹ the electronic structure of glassy transition-metal alloys is similar to that of the crystalline alloy of the same composition. The similarities justify a comparison of our experimental data for $\text{Nb}_{55}\text{Rh}_{45}$ with the state densities given by a self-consistent augmented spherical wave (ASW) band calculation for $\text{Nb}_{50}\text{Rh}_{50}$ in the CuAu structure. In Fig. 4 we show the calculated total and site-decomposed state densities at the theoretical equilibrium lattice separation. The calculations clearly show that NbRh has a common d band (the total state density is similar to that of fcc technetium⁷) and that the states at E_F are predominantly due to the Nb (early transition metal). Note that the occupied portion of the calculated d -band width is 5.4 eV while the measured band width is 5.3 eV. The Rh d -band complex consists of two peaks located at 4.1 and 1.9 eV while the measured Rh d -band complex is at 2.8 eV. The Nb d band has two peaks located at 0.7 eV and at the bottom of the valence band. Comparison of the calculated site state densities at E_F with the state densities of the pure elements at E_F explains the observed change in core-level line shape asymmetries: 0.6 states/eV atom for Rh in NbRh compared with 1.4 states/eV atom for fcc Rh metal and 1.15 states/eV atom for Nb in NbRh compared with 1.5 states/eV atom for bcc Nb metal.

The calculated charge transferred from the Nb to Rh atoms on alloying is relatively small (0.1 electron per atom) compared with other glass forming transition-metal alloys (typically 0.5 electrons per atom). The almost vanishing charge transfer is consistent with the small core-level binding-energy shift at the Rh site (Table I). From this point of view, similar small charge transfers are expected to take place in Nb-Ir, Ta-Rh, and Ta-Ir alloys, since the binding-energy shifts for Rh and Ir in these alloys are also quite small or even negative (Ir alloys).

In summary the present work shows that the

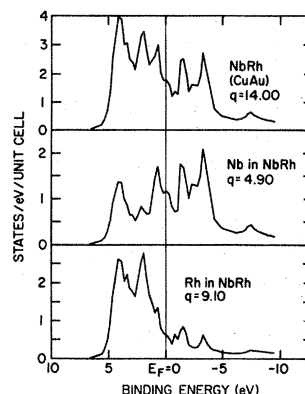


FIG. 4. Calculated, total, and site-decomposed state densities for NbRh in the CuAu structure. q is the total charge and the charge per site, respectively.

glass forming T_5T_9 alloys reveal a common d band as has been observed previously in transition-metal alloys with a valence difference of the alloy constituents of $\Delta n = 3$. A large shift of the d states related to the late transition metal to higher binding energy has been found both experimentally and theoretically. The d states of the early transition metals dominate the electronic structure near E_F and are responsible for superconductivity of these alloys since it is well known that the electrons at E_F are those involved in superconductivity. Band-structure calculations for NbRh suggest a very small charge transfer on alloying which is consistent with the small core-level binding-energy shifts observed by XPS measurements.

ACKNOWLEDGMENTS

Financial support of the Swiss National Science Foundation, the Kommission zur Förderung der wissenschaftlichen Forschung, the Eidgenössische Stiftung zur Förderung Schweizerischer Volkswirtschaft, and the Fonds für Lehre und Forschung is gratefully acknowledged. Research was sponsored in part by the Division of Materials Sciences, U.S. Department of Energy, under Contract No. W-7405-eng-26 with the Union Carbide Corporation.

*On leave from Oak Ridge National Laboratory, Oak Ridge, Tennessee 37830.

†Present address: IBM Thomas J. Watson Research Center, Yorktown Heights, New York 10598.

¹S. Davis, M. Fischer, B. C. Giessen, and D. E. Polk, in *Rapidly Quenched Metals III*, edited by B. Cantor (The Metals Society, London, 1978), Vol. 2, p. 425.

²C. C. Koch, D. M. Kroeger, J. O. Scarbrough, and B.

- C. Giessen, *Phys. Rev. B* **22**, 5213 (1980).
- ³W. L. Johnson and S. J. Poon, *J. Appl. Phys.* **46**, 1787 (1975).
- ⁴P. Oelhafen, E. Hauser, and H. -J. Güntherodt, *Phys. Rev. Lett.* **43**, 1134 (1979).
- ⁵J. H. Scofield, *J. Electron Spectrosc. Relat. Phenom.* **8**, 129 (1976).
- ⁶P. Oelhafen *et al.* (unpublished).
- ⁷V. L. Moruzzi, J. F. Janak, and A. R. Williams, *Calculated Electronic Properties of Metals* (Pergamon, New York, 1978).
- ⁸P. Oelhafen, E. Hauser, and H. -J. Güntherodt, in *Inner Shell and X-ray Physics of Atoms and Solids*, edited by D. J. Fabian, H. Kleinpoppen, and L. M. Watson (Plenum, New York, 1981), p. 575.
- ⁹B. Velický, S. Kirkpatrick, and H. Ehrenreich, *Phys. Rev.* **175**, 747 (1968).
- ¹⁰P. Oelhafen, E. Hauser, and H. -J. Güntherodt, *Solid State Commun.* **35**, 1017 (1980).
- ¹¹H. -J. Güntherodt, P. Oelhafen, R. Lapka *et al.*, in *Fourth International Conference on Liquid and Amorphous Metals*, Orsay, France, 1980 [*J. Phys. (Paris) Colloq.* **C-8**, 381 (1980)].
- ¹²L. F. Mattheiss, *Phys. Rev. B* **1**, 373 (1970).